Experimental study on the thermal response of PCM-based heat sink using structured porous material fabricated by 3D printing

Xusheng Hu, Xiaolu Gong

Experimental study on the thermal response of PCM-based heat sink using structured porous material fabricated by 3D printing

Xusheng Hu, Xiaolu Gong*
Charles Delaunay Institute, LASMIS, University of Technology of Troyes, 12 Rue Marie Curie, 10004 Troyes, France
(*) Corresponding author, gong@utt.fr

Abstract

Phase change material (PCM) based heat sink has the potential to be applied for the thermal management of electronic devices. Whereas, PCM suffers from a low thermal conductivity, which results in local overheating at the base of heat sink. To enhance thermal performance of heat sink, a structured porous material (SPM) used as thermal conductivity enhancer (TCE) is designed and fabricated, where 3D printing technique is adopted to achieve the fast and precise manufacture of SPM. The thermal response of heat sink using SPM with different porosities (80%, 85%, 90%, and 95%) is experimentally investigated at various heating power levels (8 W, 10 W, and 12 W). Results show that the use of SPM has a significant effect on thermal response of heat sink for electronic cooling system. Furthermore, the thermal behavior of heat sink can be further heightened by reducing the porosity of SPM, e.g., the heat sink using SPM with 80% porosity shows the highest enhancement ratio in all cases of present study. The increase of power level can result in the reduction of operation time of PCM-based heat sink. This study is of great significance for the design and application of SPM used in thermal management unit.

Keywords: Heat sink; Phase change material; Structured porous material; 3D printing; Thermal response

1. Introduction

In recent years, with the development in high-performance and miniaturized electronic devices, electronic component generates a large amount of heat, where this can cause the decline in work performance and reduction of operating life [1-3], e.g., for a temperature rise of 10 °C, thermal failure rate of electronic chips would be increased by 50% [4]. Therefore, thermal management has a vital role in the utilization of electronics subjected to high heat generation density. In the past few years, several studies focused on the usage of PCM in thermal management of electronics [5-7]. PCM can utilize its high latent heat of fusion to generate the required cooling effect. Moreover, the thermal management system using PCM requires a lower weight and fewer volume of equipment compared with conventional cooling system. Therefore, PCM-based heat sink as a passive cooling method has the potential to be applied in thermal management of electronics.

However, the low thermal conductivity of PCM reduces heat transfer rate of heat sink, which results in the rapid increase of base temperature of heat sink once PCM near the base subjected to heat source completely melts [8]. To overcome this disadvantage, the enhancement method of inserting the material with high thermal conductivity, namely thermal conductivity enhancer (TCE), into heat sink was developed [9, 10]. TCE was employed in various forms including high thermal conductivity additive [11-13], fin [14-16], pin-fin [17-19], metal foam [20-22], and honeycomb structure [23, 24]. Baby and Balaji [25] implemented an experimental study on temperature response of PCM-based heat sink using pin-fin and plate-fin structure. Results confirmed that use of fin was conducive to extending the operation time, and the pin-fin heat sinks showed a better behavior compared to plate-fin heat sinks. Rehman et al. [26] experimentally explored the operational performance of copper foam/PCMs heat sink. Their study focused on the effects of thermal properties of PCMs on thermal response of heat sinks. Results indicated that copper foam and PCM have positive effects on the thermal behavior of heat sinks. For heat sink subjected to different heat power, the optimum choice of PCM was different depending on its thermal properties. Rehman and Ali [27] in another experiment, mainly examined the influence of metal foam parameters (i.e., porosity and pore size) and the amount of PCM on thermal response of copper foam/paraffin based heat sink. Their results indicated that the porosities of metal foam significantly affected base temperature of heat sinks, and the increase of volume fraction of PCM can reduce base temperature.

The research literature has shown that structured porous material (SPM) as a TCE is able to augment thermal performance of PCMs. In our previous study, we designed a porous metal structure that was used as TCE to enhance the thermal performance of PCM [28]. The thermal characteristics of PCM composite were investigated using the pore-scale numerical method. The results indicated that the usage of porous material can drastically improve the thermal conductivity of PCM. Furthermore, it was found that the effective thermal conductivities of PCM embedded in porous material increase with the decrease of the porosity. Righetti et al. [29] carried out an investigation on thermal behavior of PCM infiltrated in 3D printed periodic metal

structures with various cell sizes (10 mm, 20 mm and 40 mm). They reported that the use of periodic metal structure can improve heat transfer rate of PCM in thermal energy storage system, and PCM embedded in periodic metal structure with 10 mm cell size shows the best thermal performance. Gopalan et al. [30] in a numerical investigation, used structured porous media as TEC to investigate the enhancement in thermal behavior of PCM-based heat sink, in which employed porous structure possesses various configurations including square, diamond, octahedral lattice frame, hexagonal honeycomb structure, etc. The results showed that the thermal enhancement of heat sinks using porous structure was pronounced compared with heat sink without porous structure. Moreover, they concluded that regardless of configuration of porous structure used, the effective thermal conductivity is the final and single parameter, which can determine thermal behavior of heat sinks. However, the study of thermal behavior for PCM-based heat sinks using SPM is still not enough at present.

Due to the fast development of 3D printing technique, 3D printing enables a big leap for configuration flexibility, where this provides a possibility to fast and accurately fabricate SPM [31, 32]. Structured porous material is a promising candidate to be used as TCE owing to its controlled structure (e.g., porosity, pore size and cell shape) and material (e.g., aluminum and copper) by applying 3D printing technique [33]. Therefore, the corresponding investigation on the usage of 3D printed SPM in the thermal management unit is of great significance. In this paper, selective laser melting (SLM) as a 3D printing technique was used to fabricate SPM with a cubic unit cell. The experimental investigation was conducted to understand the role of SPM on the enhancement in thermal behavior of heat sink. Meanwhile, the effects of porosity of SPM and power level of heat source on the thermal response of PCM-based heat sink were also investigated.

2. Experimental details

2.1 Sample material

There are some factors considered for the selection of phase change material, including chemical stability, latent heat, supercooling and melting point, etc. In the current study, the commercial paraffin RT 62HC was selected as PCM. The thermo-physical properties are provided by the manufacturer (Rubitherm, Germany), as summarized in Table 1. It can be seen that RT 62HC possesses considerable latent heat, which is conducive to enhancing thermal behavior of heat sink. A big change in volume during phase change has an adverse effect on the encapsulation of PCM, which limits the usage of PCM in thermal management. Therefore, the small volumetric expansion (2%) is considered another important factor for the choice of RT 62HC. Furthermore, RT 62HC has a relatively low cost (about US$ 7.5/kg). Considering the above advantages, RT 62HC was used.

Table 1

Thermo-physical properties of RT 62HC and aluminum [34, 35].

Materials	Thermal conductivity (W/m K)	Density (kg/m^3)	Specific heat (J/kg K)	Latent heat (kJ/kg)	Melting point (°C)
RT 62HC	0.2	850/840	2000	230	62-63
Aluminum	183	2670	940	-	-

A SPM with periodic cell structure was designed to be used as TCE, as described in Fig. 1. The unit cell of SPM possesses an ideal cubic shape, where metal ligament of SPM was connected at an angle of 90° as illustrated in Fig. 1(a). The length and thickness of metal ligaments are l and a. The porosity is a key parameter that can dramatically affect the thermal characteristics of material. The porosity is defined as the ratio of the open volume in the unit cell to the total unit cell volume. According to the value of l and a, the porosity ε can be determined by:

$$\varepsilon = \frac{l^3 - 12a^2 l + 16a^3}{l^3} \tag{1}$$

Based on the designed model, samples with dimensions $40\times40\times40$ mm^3 were made of aluminum alloy by using selective laser melting (one of 3D printing techniques) as displayed in Fig. 1(b). The detailed structure parameters of porous material with four different porosities can be seen in section 2.2. For the current study, aluminum alloy was selected as enhancer material owing to its high thermal conductivity, low density, corrosion resistance, and wide application in the electronic industry. The thermal properties are represented in Table 1. Due to the controllability of structure and material, the effect of 3D printed porous material as TCE on thermal response of heat sink will be investigated in this paper.

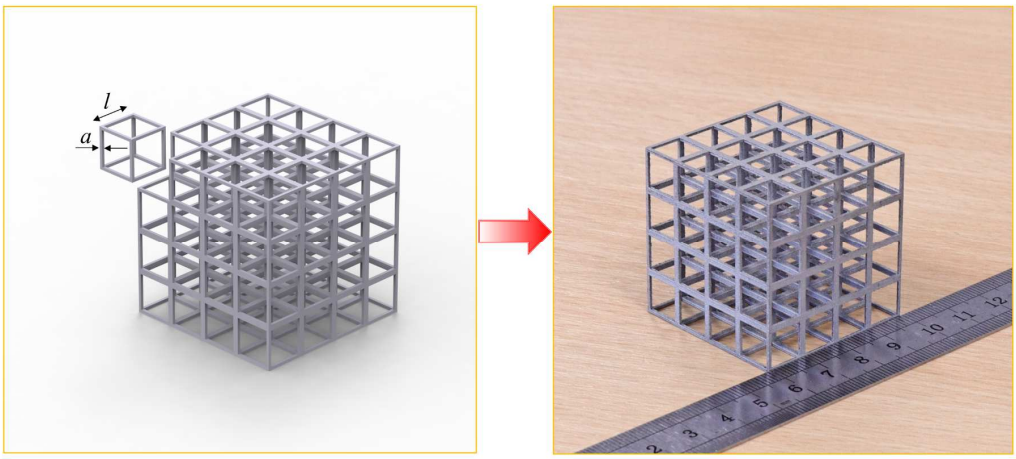

(a) (b)

Fig. 1. Porous material with cubic cell structure: (a) designed model and (b) 3D printed sample.

2.2 Experimental apparatus and procedures

A schematic diagram of experimental apparatus is presented in Fig. 2. The experimental apparatus was composed of a heating system, test section, data measurement and collection system. Constant input power can be provided to the heater via DC power, in which three various power inputs (8 W, 10 W and 12 W) were supplied to mimic the heat generation from electronic component considering different operating status of electronic devices. In data measurement and collection system, a data logger was used to record temperature data at a time interval of 1 s. Then temperature data was stored in a computer. The test section mainly consisted of heat sink, SPM, PCM, and insulation block. Six heat sinks were examined to investigate the thermal response of heat sinks with different structure for temperature control of electronic components. The configuration parameters of heat sink and SPM are summarized in Table 2.

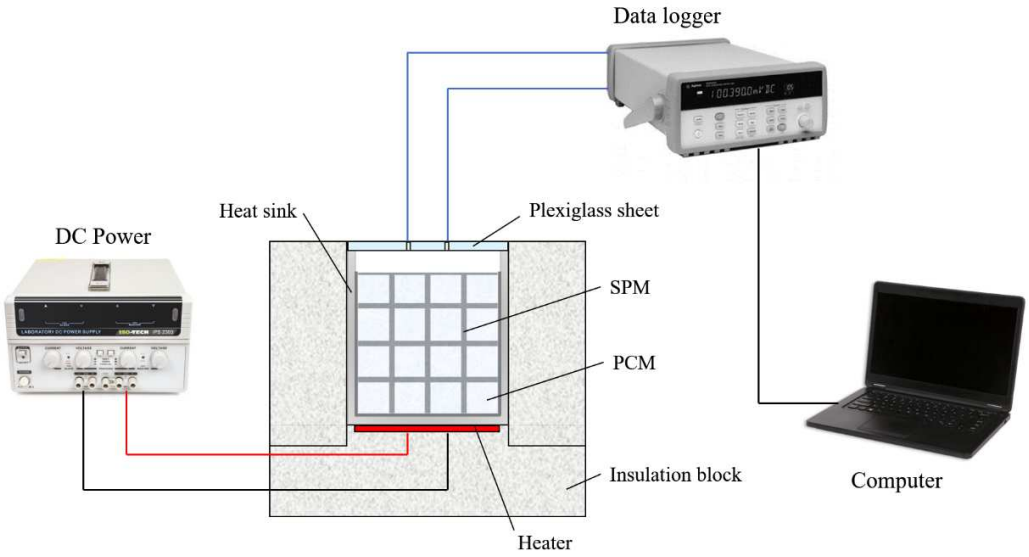

Fig. 2. Schematic diagram of experimental setup.

Table 2

Parameters of heat sink and SPM.

Heat sink Type	Dimension of heat sink $W \times L \times H$ (mm)	Porosity of SPM ε (%)	Ligament length l (mm)	Ligament thickness a (mm)
$\varepsilon = 95\%$ SPM	44 × 44 × 52	95	10	0.68
$\varepsilon = 90\%$ SPM	44 × 44 × 52	90	10	0.98
$\varepsilon = 85\%$ SPM	44 × 44 × 52	85	10	1.22
$\varepsilon = 80\%$ SPM	44 × 44 × 52	80	10	1.43
No SPM	44 × 44 × 52	-	-	-

Single heat sink	44 × 44 × 52	-	-	-

Fig. 3 clearly depicts the exploded view of test section. The insulation block with low thermal conductivity (k = 0.042 W/m K) was employed to enclose heat sink with the aim of reducing thermal loss. The heat sink with 2 mm thickness was made of aluminum slab (AL-T6-6061) using electric discharge machine (EDM). A plate heater of dimensions $40\times40\times1$ mm^3 was used for mimicking the heat generation of electronic chips, where the heater was mounted in the recess of insulation block. A thin layer of thermal grease was employed between heat sink base and heater for diminishing contact resistance. The SPM and PCM were kept in the cavity of heat sink. Taking into consideration the effect of the amount of PCM on the thermal response of heat sink, the mass of paraffin filled in heat sinks was the same and 40 g in all experiments. To observe the experiment evolution and fix thermocouples, a plexiglass sheet was utilized at the top of heat sink. Two round holes were punched in plexiglass sheet, where this was employed for fixing wires of thermocouples.

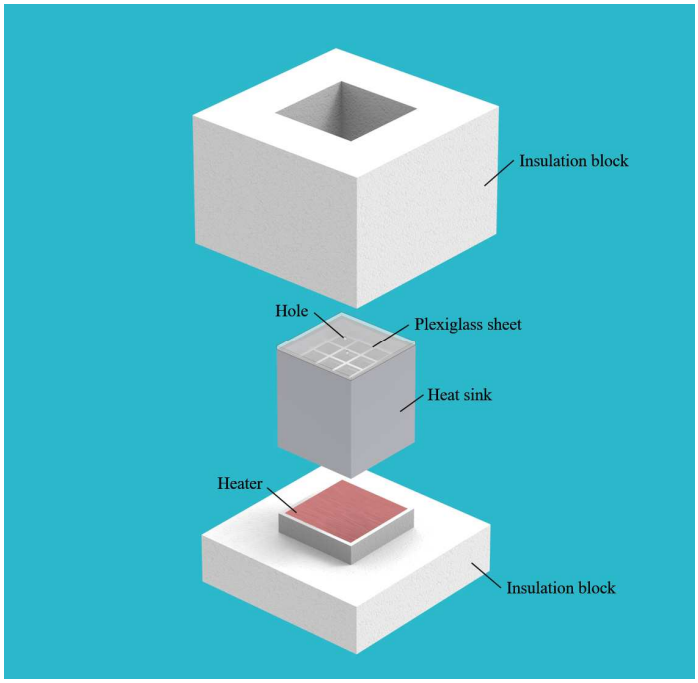

Fig. 3. Exploded view of test section.

2.3 Thermocouple positions

For the present experiment, six calibrated K-type thermocouples were employed to trace the temperature variation at the different positions of heat sink. The detailed locations of thermocouples are depicted in Fig. 4. To achieve the base temperature, three thermocouples (TC#3, TC#4, and TC#5) were evenly attached to bottom surface of heat sink along vertical centerline. The internal temperature of heat sink was measured by two thermocouples (TC#1 and TC#2) inserted into two symmetrical locations at the height of 20 mm from heat sink base. To

ensure their positions within heat sink, TC#1 and TC#2 were embedded into heat sink through round holes of plexiglass sheet, and the thermal adhesive was used for fixation of thermocouples and holes. The last thermocouple was employed for monitoring environment temperature.

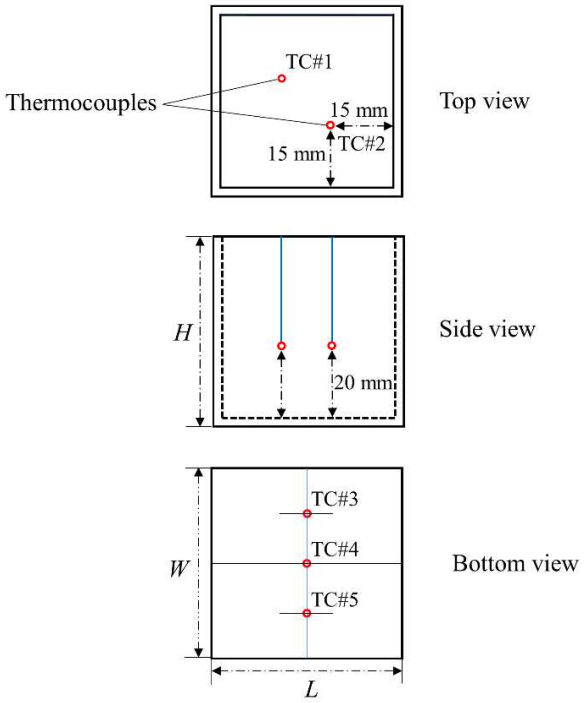

Fig. 4. Thermocouple distribution positions.

2.4 Uncertainty in measurement

The uncertainties in experiment were caused by the errors of apparatus used, containing DC power, plate heater, and thermocouple. The uncertainty of power input supplied by DC power is 1%, which can be determined using a standard calibrated multi-meter. The uncertainty of plate heater is 5%, which is provided by the manufacturer. The uncertainty of temperature measurement can be estimated by a standard thermometer. The maximum deviation in the temperature is ±0.5 ℃. Since the temperature is ranging from 20 ℃ to 90 ℃ in the current experiment, the maximum uncertainty of temperature measurement is within ±2.5%.

3. Results and discussions

To study the role of SPM on thermal enhancement of PCM based heat sink, temperature response of heat sinks with varying porosities SPM is analyzed and compared, in which the heat sink base is subjected to three different power inputs of 8 W, 10 W, and 12 W. The average value of thermocouples TC#3, TC#4, and TC#5 is used to represent the base temperature of heat sink. The base temperature acts as the maximum temperature of electronic component. Considering the allowable operational temperature of common electronic devices, the maximum value of base temperature is set to about 70 ℃ to secure operating efficiency and reliability of electronics.

Thereby, the current experiments complete when the base temperature reaches this maximum temperature.

3.1 Enhancement in the thermal performance of heat sink

Fig. 5 depicts the comparison of base temperature for single heat sink, heat sink with PCM, and heat sink with PCM and SPM at the power level 8 W. The average value of thermocouples TC#3, TC#4, and TC#5 is employed to represent base temperature of heat sink. The comparison experiment was performed under the same experimental condition, as described in section 2.2. It is seen from experimental result that ambient temperature is about 20 ℃. An allowable operating temperature of electronic component is assumed to 70 ℃. For single heat sink that is the heat sink without PCM and SPM, the base temperature has risen to 70 ℃ at 667 s. The operation time of no SPM (i.e., heat sink with PCM) is 2140 s, which is 3.2 times as much as that of single heat sink. It indicates that the use of PCM has a positive role in thermal enhancement of heat sinks. Furthermore, results show the operation time of $\varepsilon = 80\%$ SPM (i.e., heat sink with PCM and SPM) to reach allowable temperature 70 ℃ is prolonged to 4045 s, which is 6.1 times and 1.9 times that of single heat sink and heat sink with PCM, respectively. This reveals that the combined usage of PCM and SPM in heat sink can dramatically heighten the thermal behavior of heat sink.

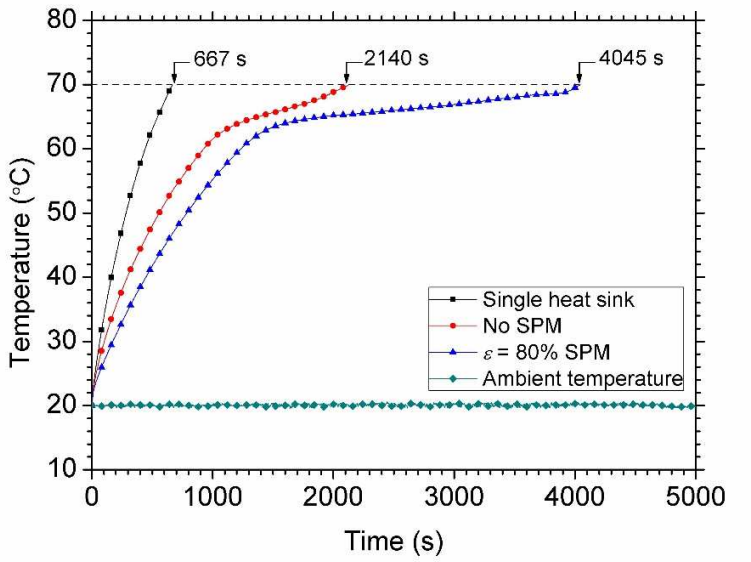

Fig. 5. Temperature response of different types heat sinks at the power level 8 W.

3.2 Effect of porosity of structured porous material

Fig. 6(a-c) shows a comparison of temperature response for heat sinks with different porosities SPM at three various power levels of 8 W, 10 W, and 12 W. Results show that the trend in temperature variation of all heat sinks is similar at different heating powers. At 8 W, the base temperature of heat sink is lower compared with that at 10 W and 12 W. The base temperature of heat sink continues to rise rapidly until paraffin within heat sink starts to melt.

The increasing rate of base temperature becomes small after paraffin near the base surface of heat sink begins to melt, which is attributed to that PCM absorbs a large amount of heat by latent heat. It is clear that the base temperature of heat sinks with SPM is lower than that of heat sink without SPM at the same time. This is owing to that heat can be rapidly removed from base to entire zone of heat sink through high thermal conductivity SPM. The maximum temperature difference between heat sink without SPM and heat sink with SPM is about 10 ℃ at the same time. This is significant for the application of PCM-based heat sink. For instance, the failure rate of electronic chips depends on the operating temperature. The reduction of 1 ℃ in operating temperature can decrease the failure rate by about 4% [36]. The base temperature of heat sinks embedding SPM with various porosities is different at any given time. This temperature diversity implies that the porosity of SPM has an important effect on thermal response of heat sinks. The heat sink using 80% porosity SPM shows the minimum rise in base temperature compared with no SPM, 85%, 90%, and 95% porosities heat sinks. Moreover, it is worth noting that the increase in input power results in the reduction of operational time of all heat sinks.

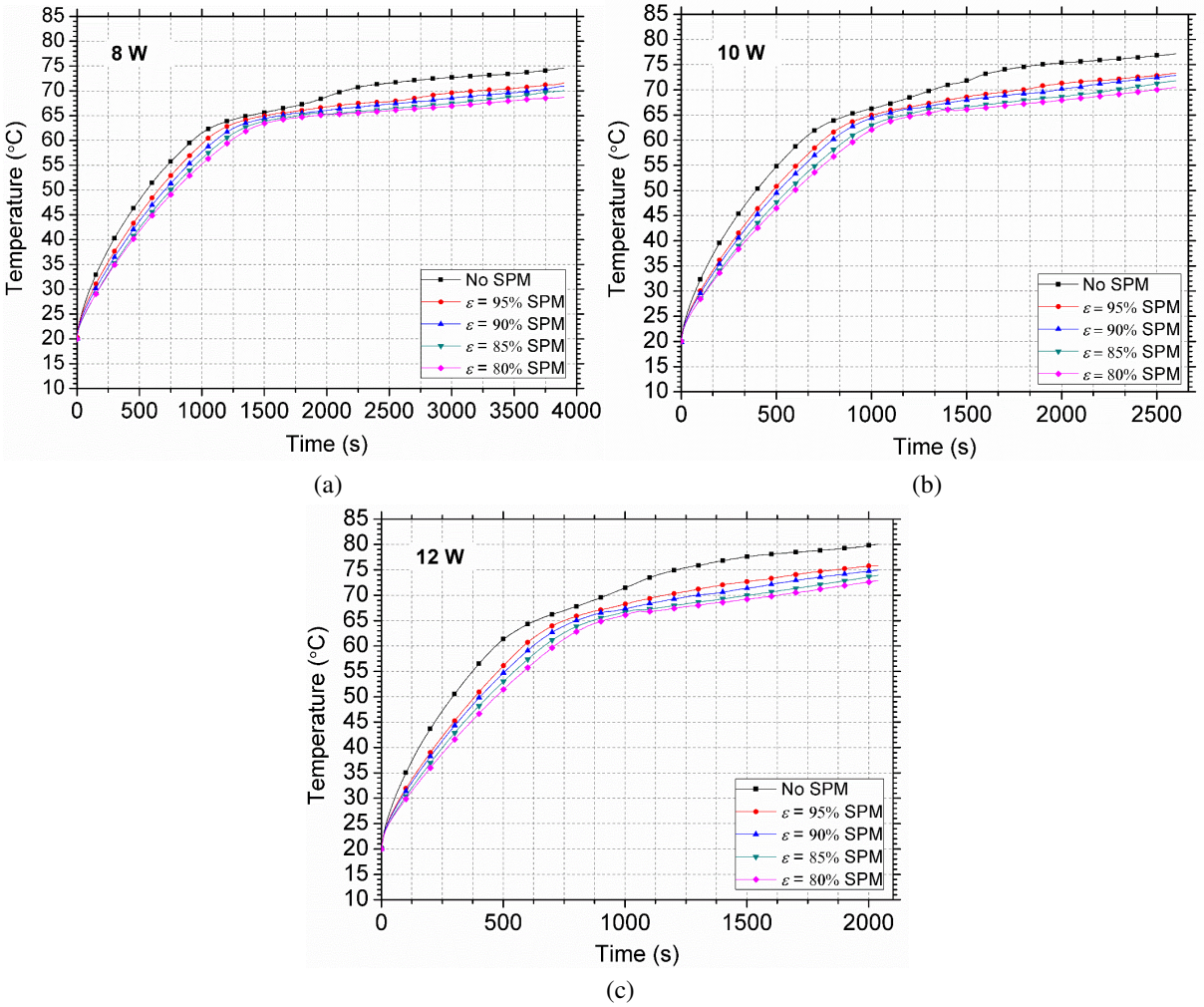

Fig. 6. Temperature response of designed heat sinks at various power levels (a) 8 W, (b) 10 W, and (c) 12 W.

3.3 Temperature variation for charging and discharging process

To further investigate the thermal behavior of heat sink, the temperature values of thermocouples fixed at different locations of heat sink are extracted, where thermocouples TC#1 and TC#2 are used to record the temperature inside heat sink. As it is seen from Fig. 6 that the heat sink with 80% porosity SPM shows the best thermal performance among all compared heat sinks. Therefore, the temperature distribution of heat sink with 80% porosity SPM during charging and discharging process is employed to show. The complete cycle process is divided into two stages, where one is charging stage and the other is discharging stage. Both the charging stage and discharging stage can be further labeled into three sub-stages depicted in Fig. 7.

In the charging stage, the rising rate of temperature is high in the pre-sensible heating and post-sensible heating stages. The temperature-time curve of heat sink is flat in the latent heating stage since a considerable amount of energy is stored into PCM. In the charging stage, the maximum temperature difference of no SPM heat sink is 20.1 ℃, which was recorded during the experiment. While the maximum temperature difference (ΔT) of SPM heat sink is 4.4 ℃, which is reduced by 78% compared to that of no SPM heat sink. It indicates that temperature distribution is more uniform within SPM heat sink in comparison to no SPM heat sink. In the discharging stage, it is seen that temperature decreases rapidly after input power is stopped. In the latent cooling stage, the temperature variation of heat sink is not apparent. When the solidification of PCM almost complete (i.e., post-sensible cooling), the rate of decrease in temperature is larger again.

From the results of the temperature distribution, it is found that the temperature of base is larger than that of TC#1 and TC#2 in the discharging stage. The temperature of heat sink base reaches the melting point faster as compared to that at TC#1 and TC#2 locations. This implies that the melting of PCM close to the base is earlier. In the discharging process, the base temperature is smaller than that of TC#1 and TC#2, which is owing to the heat loses from the base to the insulation block. Furthermore, it can be observed that the temperature variations at TC#1 and TC#2 points are almost the same during the charging and discharging process. This phenomenon is due to the thermocouples TC#1 and TC#2 are symmetrically inserted in heat sink and at the same height of 20 mm from the base.

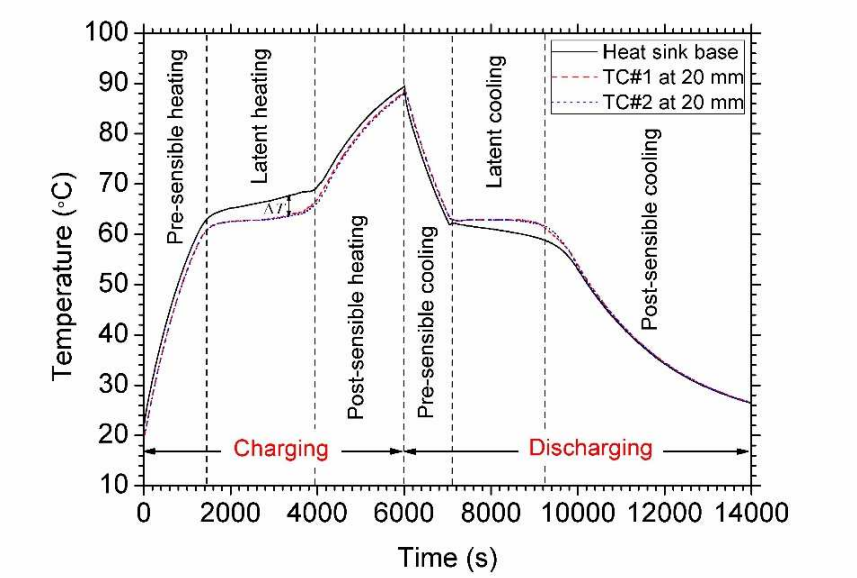

Fig. 7. Temperature profile of heat sink with 80% porosity SPM at different locations for power input of 8 W.

3.4 Enhancement in the operating time of heat sink

To evaluate role of SPM on thermal enhancement of PCM-based heat sinks, time taken by heat sinks with different configurations to reach three critical temperatures (i.e., 60 ℃, 65 ℃, and 70 ℃) is summarized in Table 3 for power inputs of 8 W, 10 W, and 12 W. The critical temperature selected represents the maximum allowable temperature of the electronic component to ensure its operational reliability. Column charts depicted in Fig. 8 (a) and (b) show the time required to critical temperatures of 60 ℃ and 70 ℃. As can be seen, operating time is varying from 469 s to 4045 s, which reflects that the embedding SPM and power level can obviously affect the thermal response of heat sinks. Results represent that the time taken by all heat sinks with SPM is larger than that of heat sink without SPM, e.g., the operation time of 95% SPM heat sink for T_{cr} = 70 ℃ increases by 50% at the heating power of 8 W in comparison with no SPM heat sink. It indicates that using SPM can effectively heighten thermal behavior of heat sinks. A notable feature among heat sinks with SPM is that the operation time of heat sink using low porosity SPM is larger. It is clear that the heat sink with 80% porosity SPM takes more time to reach each critical temperature as compared with all other heat sinks. This phenomenon implies that the reduction of porosity can better heighten the cooling performance of heat sinks. Furthermore, results show that the increase in heat generation density of electronic devices can lead to the decrease of operation time, e.g., the operating time of 80% porosity SPM heat sink at critical temperature 70 ℃ is 4045 s, 2495 s, and 1622 s for input power 8 W, 10 W, and 12 W.

Table 3

Summary sheet of time (s) required to reach various critical temperatures.

Type of	Time for T_{cr} = 60 °C			Time for T_{cr} = 65 °C			Time for T_{cr} = 70 °C		
heat sinks	8 W	10 W	12 W	8 W	10 W	12 W	8 W	10 W	12 W
No SPM	923	637	469	1371	882	631	2140	1320	925
ε = 95% SPM	1031	746	583	1509	1004	750	3211	1784	1159
ε = 90% SPM	1108	794	622	1625	1055	798	3628	1978	1292
ε = 85% SPM	1171	866	668	1769	1179	867	3884	2290	1508
ε = 80% SPM	1233	915	711	1896	1245	912	4045	2495	1622

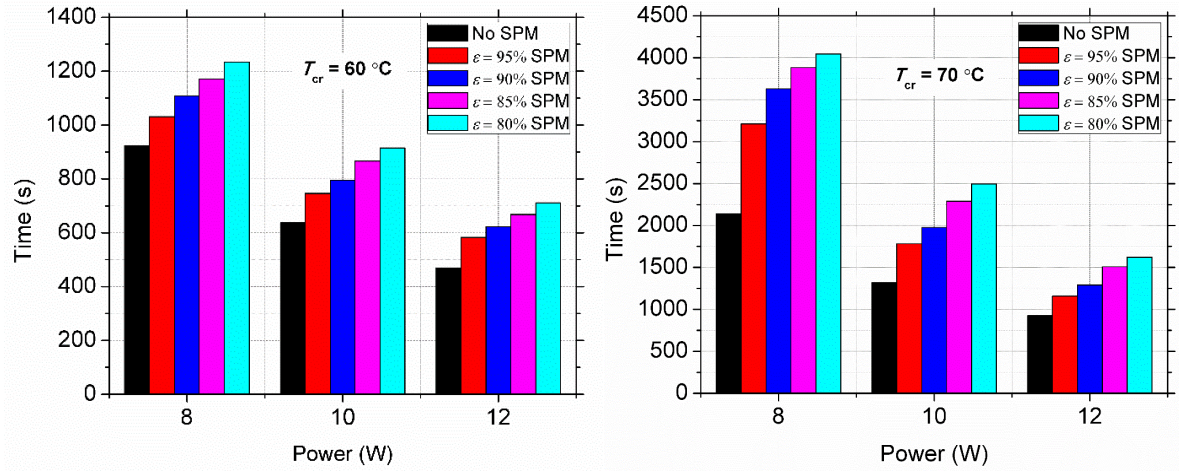

(a) (b)

Fig. 8. Time taken by various heat sinks to reach critical temperatures (a) 60 °C and (b) 70 °C.

3.5 Enhancement ratio of heat sinks with SPMs of different porosities

The enhancement in thermal behavior of heat sinks can be estimated by the enhancement ratio e_r which is the ratio of time taken by heat sink with SPM to that of heat sink without SPM to reach the critical temperature, as given in Eq. (2):

$$e_r = \frac{t_{cr}(\text{with SPM})}{t_{cr}(\text{without SPM})} \tag{2}$$

Where t_{cr} is the time required to reach the critical temperature.

The enhancement ratio of heat sink using varying porosities SPMs at the critical temperatures of 60 °C, 65 °C, and 70 °C is illustrated in Fig. 9(a-c). It is found that the heat sink using SPM with 80% porosity has the highest enhancement ratio against other heat sinks in all cases. The enhancement ratio increases with the reduction of porosity of SPM in case of using SPM, e.g., for critical temperature 70 °C, the enhancement ratios of heat sink with 95%, 90%, 85%, and 80% porosities SPMs are 1.35, 1.50, 1.73, and 1.89 at 10 W input power. It reveals that

the porosity of SPM (i.e., the volume fraction of enhancer material) has an obvious influence on thermal enhancement of PCM-based heat sink.

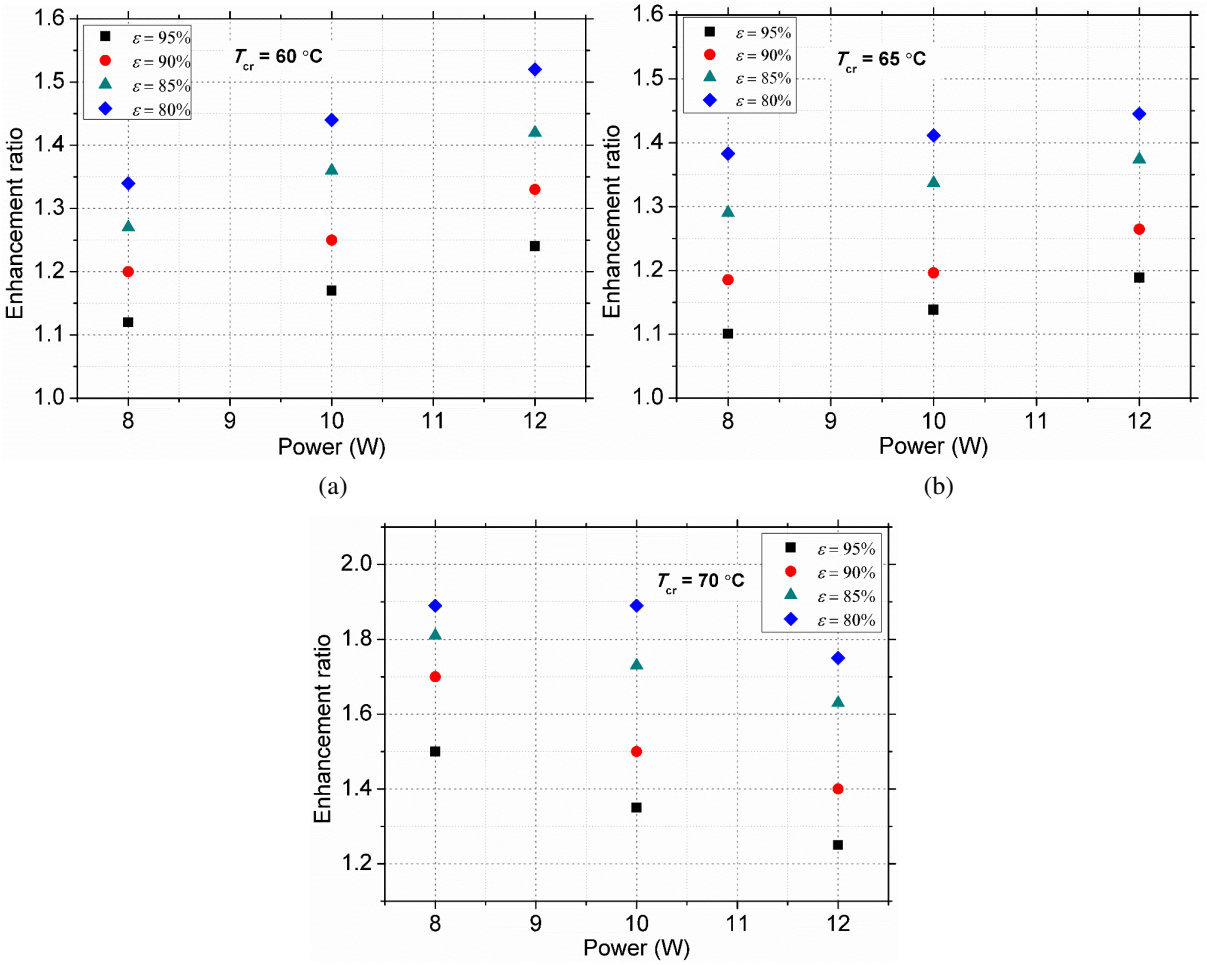

Fig. 9. Enhancement ratio of heat sinks using SPMs of various porosities for three critical temperatures of (a) 60 ℃, (b) 65 ℃, and (c) 70 ℃.

As it reveals the heat sink using SPM with 80% porosity has the highest enhancement ratio, Fig. 10 presents the comparison of enhancement ratios of 80% porosity heat sink for various critical temperatures of 60 ℃, 65 ℃, and 70 ℃. Results show the higher ratios are obtained at the critical temperature of 70 ℃ for each input power. This phenomenon is attributed to that the heat transfer between PCM and SPM is enhanced owing to the occurrence of natural convection when the critical temperature is higher than the fusion point of PCM. In the latent heating stage, heat sink using SPM can remain a longer operating time to achieve a more efficient cooling for the higher critical temperature. The enhancement ratio of SPM heat sink increases as power density increases for the critical temperatures of 60 ℃ and 65 ℃. While the enhancement ratio slightly reduces with an increase in input power for the critical temperature of 70 ℃. It reflects that the allowable operating temperature and heat generation density of electronic devices have a

comprehensive effect on the thermal response of PCM-based heat sink using SPM.

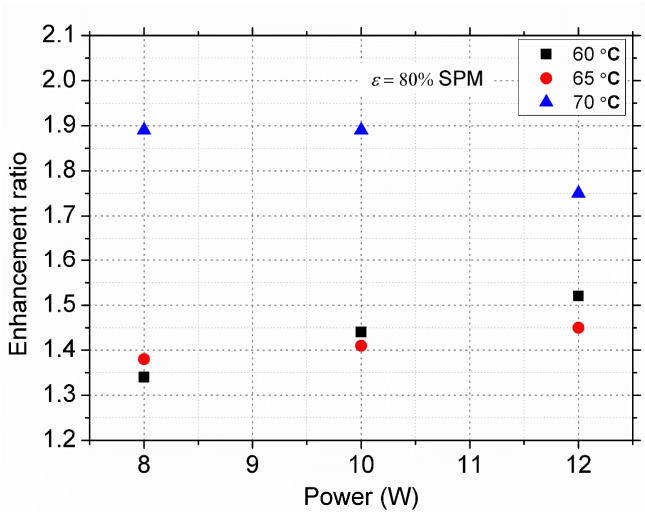

Fig. 10. Comparison of enhancement ratio for heat sink with 80% porosity SPM at three critical temperatures.

4. Conclusion

In this paper, a structured porous material with cubic unit cell was designed, and SPMs with various porosities were fabricated by 3D printing. The experiment was performed to examined the thermal response of PCM-based heat sink using SPM. Results show that the use of SPM can effectively prolong the operation time of PCM-based heat sink for electronic devices cooling. The temperature distribution is also more uniform for heat sinks using SPM. For instance, the temperature difference within heat sink using SPM with 80% porosity reduces by 78% in comparison with heat sink without SPM at power level of 8 W. It is observed from results that the porosity of SPM has an obvious influence on the effectiveness of PCM-based heat sink. The operation time of SPM heat sink increases as the porosity of SPM decreases at three power levels. The enhancement ratios of heat sinks using SPM also increase with the reduction of porosity of SPM. The heat sink using 80% porosity SPM shows the best thermal performance in all cases of current experiments. In addition, heating power level also affects the thermal response of SPM PCM-based heat sink. The increase of power level can result in the reduction of operation time of PCM-based heat sink.

Acknowledgement

This work was supported by China Scholarship Council.

References

[1] A.L. Moore, L. Shi, Emerging challenges and materials for thermal management of electronics, Mater. Today 17 (2014) 163-174.

[2] C.X. Wang, L.J. Hua, H.Z. Yan, B.J. Li, Y.D. Tu, R.Z. Wang, A Thermal Management Strategy for Electronic Devices Based on Moisture Sorption-Desorption Processes, Joule 4

(2020) 435-447.
[3] E.M. Abo-Zahhad, S. Ookawara, A. Radwan, M.F. Elkady, A.H. El-Shazly, Optimization of stepwise varying width microchannel heat sink for high heat flux applications, Case Studies in Thermal Engineering 18 (2020) 100587.
[4] A. Vassighi, M. Sachdev, Thermal and power management of integrated circuits, 2006 ed., Springer, New York, 2006.
[5] S. Gharbi, S. Harmand, S. Ben Jabrallah, Experimental comparison between different configurations of PCM based heat sinks for cooling electronic components, Appl. Therm. Eng. 87 (2015) 454-462.
[6] M. Emam, S. Ookawara, M. Ahmed, Thermal management of electronic devices and concentrator photovoltaic systems using phase change material heat sinks: Experimental investigations, Renewable Energy 141 (2019) 322-339.
[7] X.H. Yang, S.C. Tan, Z.Z. He, Y.X. Zhou, J. Liu, Evaluation and optimization of low melting point metal PCM heat sink against ultra-high thermal shock, Appl. Therm. Eng. 119 (2017) 34-41.
[8] K.C. Nayak, S.K. Saha, K. Srinivasan, P. Dutta, A numerical model for heat sinks with phase change materials and thermal conductivity enhancers, Int. J. Heat Mass Transfer 49 (2006) 1833-1844.
[9] S.S. Feng, M. Shi, Y.F. Li, T.J. Lu, Pore-scale and volume-averaged numerical simulations of melting phase change heat transfer in finned metal foam, Int. J. Heat Mass Transfer 90 (2015) 838-847.
[10] R. Baby, C. Balaji, Experimental investigations on thermal performance enhancement and effect of orientation on porous matrix filled PCM based heat sink, International Communications in Heat and Mass Transfer 46 (2013) 27-30.
[11] S. Ramakrishnan, X. Wang, J. Sanjayan, Effects of various carbon additives on the thermal storage performance of form-stable PCM integrated cementitious composites, Appl. Therm. Eng. 148 (2019) 491-501.
[12] S. Ramakrishnan, X. Wang, J. Sanjayan, J. Wilson, Heat Transfer Performance Enhancement of Paraffin/Expanded Perlite Phase Change Composites with Graphene Nano-platelets, Energy Procedia 105 (2017) 4866-4871.
[13] Q. Ren, F. Meng, P. Guo, A comparative study of PCM melting process in a heat pipe-assisted LHTES unit enhanced with nanoparticles and metal foams by immersed boundary-lattice Boltzmann method at pore-scale, Int. J. Heat Mass Transfer 121 (2018) 1214-1228.
[14] S.K. Saha, K. Srinivasan, P. Dutta, Studies on Optimum Distribution of Fins in Heat Sinks Filled With Phase Change Materials, J. Heat Transfer 130 (2008).
[15] A.M. Abdulateef, J. Abdulateef, K. Sopian, S. Mat, A. Ibrahim, Optimal fin parameters used for enhancing the melting and solidification of phase-change material in a heat exchanger unite, Case Studies in Thermal Engineering 14 (2019) 100487.

[16] A.K. Hassan, J. Abdulateef, M.S. Mahdi, A.F. Hasan, Experimental evaluation of thermal performance of two different finned latent heat storage systems, Case Studies in Thermal Engineering 21 (2020) 100675.
[17] A. Arshad, H.M. Ali, S. Khushnood, M. Jabbal, Experimental investigation of PCM based round pin-fin heat sinks for thermal management of electronics: Effect of pin-fin diameter, Int. J. Heat Mass Transfer 117 (2018) 861-872.
[18] R. Baby, C. Balaji, Thermal optimization of PCM based pin fin heat sinks: An experimental study, Appl. Therm. Eng. 54 (2013) 65-77.
[19] X. Yang, P. Wei, G. Liu, Q. Bai, Y.-L. He, Performance evaluation on the gradient design of pore parameters for metal foam and pin fin-metal foam hybrid structure, Appl. Therm. Eng. 175 (2020) 115416.
[20] A. Atal, Y. Wang, M. Harsha, S. Sengupta, Effect of porosity of conducting matrix on a phase change energy storage device, Int. J. Heat Mass Transfer 93 (2016) 9-16.
[21] X. Hu, F. Zhu, X. Gong, Experimental and numerical study on the thermal behavior of phase change material infiltrated in low porosity metal foam, J. Energy Storage 26 (2019) 101005.
[22] H. Xu, Y. Wang, X. Han, Analytical considerations of thermal storage and interface evolution of a PCM with/without porous media, International Journal of Numerical Methods for Heat & Fluid Flow 30 (2019) 373-400.
[23] S. Mahmoud, A. Tang, C. Toh, R. AL-Dadah, S.L. Soo, Experimental investigation of inserts configurations and PCM type on the thermal performance of PCM based heat sinks, Appl. Energy. 112 (2013) 1349-1356.
[24] B. Xie, W.L. Cheng, Z.M. Xu, Studies on the effect of shape-stabilized PCM filled aluminum honeycomb composite material on thermal control, Int. J. Heat Mass Transfer 91 (2015) 135-143.
[25] R. Baby, C. Balaji, Experimental investigations on phase change material based finned heat sinks for electronic equipment cooling, Int. J. Heat Mass Transfer 55 (2012) 1642-1649.
[26] Tauseef-ur-Rehman, H.M. Ali, A. Saieed, W. Pao, M. Ali, Copper foam/PCMs based heat sinks: An experimental study for electronic cooling systems, Int. J. Heat Mass Transfer 127 (2018) 381-393.
[27] Tauseef-ur-Rehman, H.M. Ali, Experimental investigation on paraffin wax integrated with copper foam based heat sinks for electronic components thermal cooling, International Communications in Heat and Mass Transfer 98 (2018) 155-162.
[28] X. Hu, X. Gong, Pore-scale numerical simulation of the thermal performance for phase change material embedded in metal foam with cubic periodic cell structure, Appl. Therm. Eng. 151 (2019) 231-239.
[29] G. Righetti, G. Savio, R. Meneghello, L. Doretti, S. Mancin, Experimental study of phase change material (PCM) embedded in 3D periodic structures realized via additive manufacturing, International Journal of Thermal Sciences 153 (2020) 106376.

[30] K.S. Gopalan, V. Eswaran, Numerical investigation of thermal performance of PCM based heat sink using structured porous media as thermal conductivity enhancers, International Journal of Thermal Sciences 104 (2016) 266-280.
[31] T.D. Ngo, A. Kashani, G. Imbalzano, K.T.Q. Nguyen, D. Hui, Additive manufacturing (3D printing): A review of materials, methods, applications and challenges, Composites Part B: Engineering 143 (2018) 172-196.
[32] A. Maiti, W. Small, J.P. Lewicki, T.H. Weisgraber, E.B. Duoss, S.C. Chinn, M.A. Pearson, C.M. Spadaccini, R.S. Maxwell, T.S. Wilson, 3D printed cellular solid outperforms traditional stochastic foam in long-term mechanical response, Scientific reports 6 (2016) 24871.
[33] G. Singh, P.M. Pandey, Uniform and graded copper open cell ordered foams fabricated by rapid manufacturing: surface morphology, mechanical properties and energy absorption capacity, Materials Science and Engineering: A 761 (2019) 138035.
[34] Rubitherm GmbH, Data sheet, Rubitherm Technologies GmbH, Berlin, Germany, 2018.
[35] X. Hu, X. Gong, Experimental and numerical investigation on thermal performance enhancement of phase change material embedding porous metal structure with cubic cell, Appl. Therm. Eng. 175 (2020) 115337.
[36] S.F. Hosseinizadeh, F.L. Tan, S.M. Moosania, Experimental and numerical studies on performance of PCM-based heat sink with different configurations of internal fins, Appl. Therm. Eng. 31 (2011) 3827-3838.